SLAC-PUB-95-6987
August 1995

Polarization studies of strained GaAs photocathodes at the SLAC Gun Test Laboratory*

CONF-9505/2--

P.Sáez, R. Alley, J. Clendenin, J. Frisch, R. Kirby, R. Mair, T. Maruyama, R. Miller, G. Mulhollan, C. Prescott, H. Tang and K. Witte

Stanford Linear Accelerator Center
Stanford University, Stanford, CA 94309

ABSTRACT

The SLAC Gun Test Laboratory apparatus, the first two meters of which is a replica of the SLAC injector, is used to study the production of intense, highly–polarized electron beams required for the Stanford Linear Collider and future linear colliders. The facility has been upgraded with a Mott polarimeter in order to characterize the electron polarization from photocathodes operating in a DC gun. In particular, SLAC utilizes *p*-type, biaxially-strained GaAs photocathodes which have produced longitudinal electron polarizations greater than 80% while yielding pulses of 5 A/cm^2 at an operating voltage of 120 kV. Among the experiments performed include studying the influences of the active layer thickness, temperature, quantum efficiency and cesiation on the polarization. The results might help to develop strained photocathodes with higher polarization.

I. INTRODUCTION

The Stanford Linear Accelerator Center (SLAC) conducts experiments in high-energy physics to study the structure of elementary particles. Recent experiments have required high-intensity, high-polarization electron beams. Advances in III-V semiconductors have led to photocathodes which produce beams with polarization in excess of 80%.

The Gun Test Laboratory was created to study guns and photocathodes for the SLAC injector and the Next Linear Collider project. Of particular interest in this work has been to investigate the polarization dependence on cathode thickness, temperature, quantum efficiency (QE) and cesiation. The results of these experiments have shed light on understanding semiconductor properties which will aid us to develop better photocathodes for future experiments.

II. APPARATUS

A schematic of the Gun Test Laboratory apparatus is shown in Fig. 1. The injector section includes an ultra-high-vacuum, high-voltage electrostatic gun, a load-lock chamber for cathode transfer and activation (not shown in Fig.1), a beamline with magnetic components for electron beam transport, and several instruments for steering and characterizing the beam [1]. The gun consists of a pair of

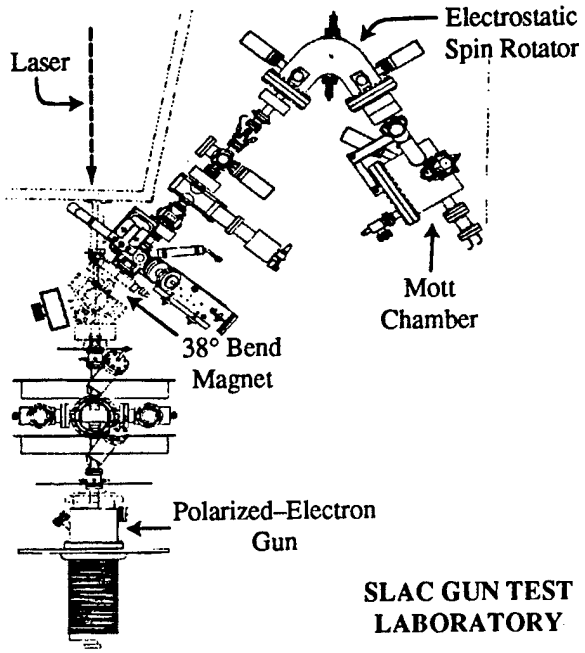

FIG. 1. Schematic of the Gun Test Laboratory apparatus.

cylindrical Pierce electrodes with a 20 mm diameter photocathode. The cathode is normally biased at -120 kV. After transport beyond the bend, the beam is injected into the recently commissioned Mott beamline [2]. This section includes an electrostatic spin rotator and a Mott scattering chamber with two CaF_2(Eu) scintillator detectors located 120° with respect to the incident beam axis. The Mott–scattering target is 700 Å gold on 1.3 μm carbon backing.

The light for electron photoemission is provided by two independent Ti:Sapphire cavities which are pumped by a pulsed Nd:YAG laser [1]. The cavities are not designed for rapid tuning of the wavelength, thus limiting each experiment to at most two wavelengths. Each pulse is 2 ns FWHM. A Pockels cell is used to produce >99% circularly-polarized light, reversible from pulse to pulse.

The polarimeter calibration was performed with a 'standard' photocathode whose polarization has been measured by highly accurate instruments [2,3]. The absolute uncertainty of the polarization measurements is ~5%, expected to become ~3%. The cathodes studied include a 100 nm active–layer (110) GaAs (C1), 100 nm strained–active–layer (100) GaAs (C2) and a bulk (100) GaAs (C3). The biaxial–compressive stress in C2 is obtained by growing GaAs on $GaAs_{0.72}P_{0.28}$ which has a lattice constant

* Work supported by Department of Energy contract DE-AC03-76SF00515.

Presented at the 16th IEEE Particle Accelerator Conference (PAC 95) and International Conference on High Energy Accelerators, Dallas, Texas, May 1-5, 1995.

DISCLAIMER

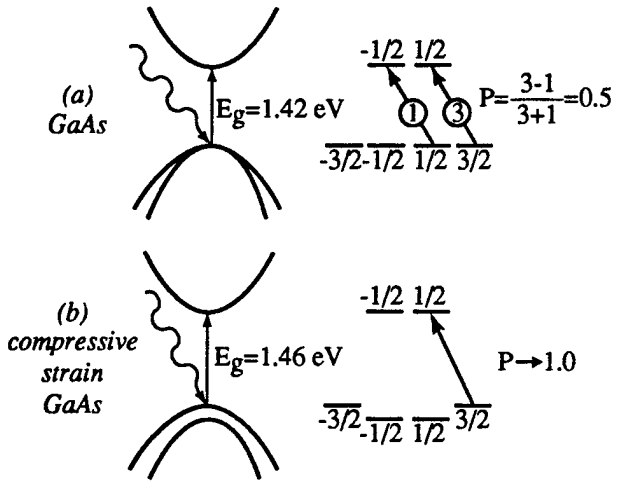

FIG. 2. Energy-band diagrams of the electromagnetic transitions at the Γ point for (a) GaAs and (b) strained GaAs. The polarization corresponds to excitation of valence band states by left–circularly-polarized illumination. The circled numbers indicate the relative transition strengths.

approximately 1% smaller than bulk GaAs [4]. C1 and C2 are doped to 5×10^{18} cm^{-3} while C3 is doped to 2×10^{19} cm^{-3}. The electromagnetic transitions that lead to electron beam polarization are shown in Fig. 2.

III. RESULTS

Several conduction band spin–relaxation effects take place in the bulk of a semiconductor [5,6]. Electron depolarization as a function of material thickness has been observed previously and has prompted the use of thin samples [7]. Thus the higher room–temperature polarization of C1 (P=44%) over C3 (P=29%) is brought about by reduced travel time of electrons in the semiconductor.

Large improvements in polarization from bulk materials brought by lower temperatures [8] led us to investigate the possibility of existence of this effect in C1 and C2. Figure 3 shows a plot of C2's polarization as a function of temperature. The small improvement in P indicates that spin relaxation mechanisms, which typically have strong temperature dependencies [6], do not play a major role in the depolarization of electrons from thin materials.

To see how temperature affects the spin orientation of electrons in thin samples, consider the electron polarization in the conduction band at the time of recombination

$$P = \frac{P_0}{1+\frac{\tau}{\tau_s}} \qquad (1)$$

where P_0 is the initial electron polarization, τ is its lifetime in the conduction band and τ_s is the spin–relaxation time. Strictly speaking, Eqn. (1) applies to the ideal photoluminescence experiment; however, it can be used to *approximate* the spin orientation of a photoemitted electron. (A complete model for

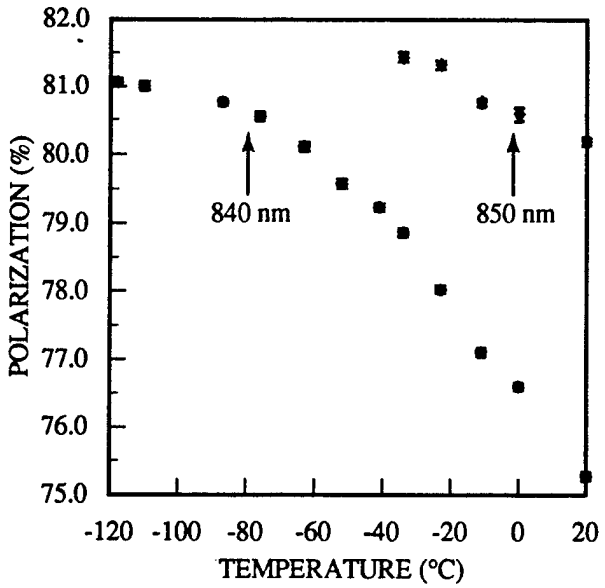

FIG. 3. Electron polarization versus temperature for 100 nm strained GaAs (p–doped to 5×10^{18} cm^{-3}). Two wavelengths were used to track the increase in bandgap with lower temperatures. Peak polarization at low temperatures increases by ~1% from its room– temperature value.

the polarization of a photoemitted electron would include light absorption, diffusion to the surface, and emission from the band–bending/surface region.) The travel time of a thermalized electron in 100 nm in the absence of collisions is about 2.5×10^{-13} s ($\langle v\rangle\approx4\times10^{7}$ cm/s at room temperature [9]). Such time is already much smaller than the spin–relaxation time $\tau_s\sim2\times10^{-11}$ s [6]. Substitution into Eqn. (1) of a considerably longer spin–relaxation time due to lower temperatures increases the electron polarization by only 2%.

After cesiating a photocathode beyond its photoemission peak, the QE and polarization will have dropped as shown in Fig. 4. This excess cesium might contribute to depolarization [11]. As the cesium state on the surface of the photocathode changes with time, the QE and polarization improves. However, when the surface conditions worsen, the QE drops but the polarization keeps improving. This polarization dependence on QE, with lower QEs yielding higher polarizations, has been seen before [1,8]. This effect is larger on strained samples like C2 ($\Delta P/P\sim5\%$) than on unstrained samples like C1 ($\Delta P/P\sim1\%$). As the QE decreases, the rise of the work function helps to filter out those electrons that have lost energy due to scattering during their trip (or trips, in the case of reflected electrons) to the surface. These electrons might have lower polarization than ballistic electrons.

The stronger dependence of polarization on QE in strained samples is due to their broad–band configuration. The lack of well-defined, split–$P_{3/2}$ states is caused by partial strain relaxation [10]. The combination of various stages of strain relaxation results in electrons higher in the broad conduction band having higher polarizations than those at the very bottom of the band [2]. As the surface degrades with time, the rising work function prevents low conduction band

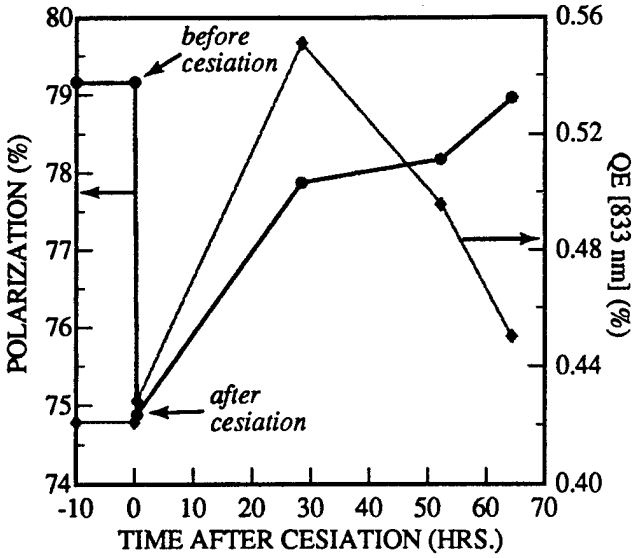

FIG. 4. Polarization and QE after cesiation for strained GaAs. The large drop in P is due to the new cesium on the surface. Also shown is the rise of P as the QE decreases.

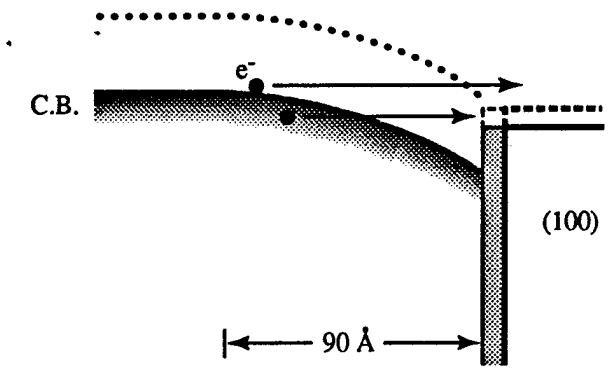

FIG. 5. Surface band diagram showing the filtering of low–conduction–band electrons by a rising work function. The (100) GaAs band–bending is 0.3 eV at the surface and 90 Å wide for p–type doping of 5×10^{18} cm^{-3}. The upper dotted line represents the upper–conduction–band L-valley which is responsible for reflections at the surface.

electrons from escaping. Such an effect is shown in Fig. 5.

IV. DISCUSSION

The lower polarization in thin (110) GaAs (P=44% instead of P=50%) and its weak dependence on temperature might indicate that the source of depolarization is not in the bulk but in the surface/band–bending region instead. A polarization dependence on crystal orientation has been observed before [12]. The crystal orientation and surface composition determine the density of surface states and the amount of band-bending [13]. In cases with large band–bending, the electron can be reflected at the surface due to its interaction with the L–valley in the conduction band [9,14]. (The L-valley is shown as the upper dotted line in Fig. 5.) During the repeated attempts at escape in the band–bending region, the electron can recombine with surface states or the valence band, loose energy through scattering and become unable to escape, and suffer spin relaxation. In addition, large electron kinetic energies in the band-bending region are thought to increase the probability of spin relaxation [15].

A (111B) surface (arsenic terminated), on the other hand, has much less band-bending (0.1 eV at the surface and 50 Å wide) which leads to lower probability of electron reflection and lower scattering in the band–bending region. Hence the probability of escape is higher and less depolarization is expected. Fortunately, the valence band splitting of (111) strained samples is similar to that of (100) samples [16]. A strained (111B) GaAs sample could be the next step towards higher polarization and higher QE photocathodes.

V. CONCLUSION

Experiments in the upgraded Gun Test Laboratory have illustrated the behavior of photocathodes under various conditions. A thin active region minimizes the travel time of electrons in the conduction band and thus reduces the effect of depolarization mechanisms. It was shown that low temperatures do not greatly improve the polarization in thin photocathodes. The 10% lower polarization than theoretically expected in thin, unstrained (110) GaAs could indicate that depolarization mechanisms occur instead in the band-bending/surface region. Strained (111B) GaAs seems like a promising material for higher polarization and QE because of its small band-bending region.

REFERENCES

[1] R. Alley *et al.*, SLAC-PUB-95-6489; submitted to Nucl. Instr. and Meth. (1995).

[2] P. Sáez, Ph.D. dissertation, Stanford University, Stanford, CA, in progress.

[3] G. Mulhollan *et al.*, these proceedings.

[4] T. Maruyama *et al.*, Phys. Rev. B **46**, 4261 (1992).

[5] G. Fishman and G. Lampel, Phys. Rev. B **16**, 820 (1977).

[6] G. Pikus and A. Titkov, in *Optical Orientation*, edited by F. Meier and B. Zakharchenya, (North-Holland, Amsterdam, 1984), Ch. 3.

[7] T. Maruyama *et al.*, Appl. Phys. Lett. **55**, 1686 (1989).

[8] D. Pierce *et al.*, Rev. Sci. Instr. **51**, 478 (1980).

[9] M. Clark, J. Phys. D: Appl. Phys. **9**, 2139 (1976).

[10] H. Aoyagi *et al.*, Phys. Lett. A **167**, 415 (1992).

[11] F. Meier, D. Pescia and M. Baumberger, Phys. Rev. Lett. **49**, 747 (1982).

[12] S. Alvarado *et al.*, Z. Phys. B - Condensed Matter **44**, 259 (1981).

[13] L. James *et al.*, J. Appl. Phys. **42**, 4976 (1971).

[14] M. Burt and J. Inkson, J. Phys. D:Appl. Phys. **10**, 721 (1977).

[15] H. Riechert, H.-J. Drouhin and C. Hermann, Phys. Rev. B **38**, 4136 (1988).

[16] F. Pollak and M. Cardona, Phys. Rev. **172**, 816 (1968).

Report Number (14) SLAC-PUB--95-6987
CONF-950512--

Publ. Date (11) 199508
Sponsor Code (18) DOE/ER, XF
UC Category (19) UC-400, DOE/ER

DOE